Investigation on high-order cascaded parametric processes in terahertz parametric oscillator with a noncollinear phase-matching scheme

Li Zhongyang[1], Zhang Yunpeng[1], Bing Pibin[1], Yuan Sheng[1], Xu Degang[2], Yao Jianquan[2]

(1. School of Electric Power, North China University of Water Resources and Electric Power, Zhengzhou 450045, China;
2. Institute of Laser and Opto-electronics, College of Precision Instrument and Opto-electronics Engineering, Tianjin University, Tianjin 300072, China)

Abstract: Cascaded optical parametric processes in terahertz parametric oscillator with a noncollinear phase-matching scheme based on bulk lithium niobate were observed. The spectra of the first−, second−, and third-order Stokes waves were observed. By analyze the spectra of the first−, second−, and third-order Stokes waves it is found that the frequency difference between adjacent-order Stokes waves is approximately equivalent, which means that the high-order cascaded parametric processes have realized. With high-order cascaded terahertz parametric processes one pump photon can generate several THz photons, which means that the quantum conversion efficiency can be enhanced.

Key words: terahertz wave; terahertz wave parametric oscillator; cascaded optical parametric oscillation

CLC number: TN24; O437 **Document code:** A **Article ID:** 1007−2276(2015)03−0990−06

非共线相位匹配太赫兹波参量振荡器级联参量过程的研究

李忠洋[1],张云鹏[1],邴丕彬[1],袁 胜[1],徐德刚[2],姚建铨[2]

(1. 华北水利水电大学 电力学院,河南 郑州 450045;
2. 天津大学 精密仪器与光电子工程学院 激光与光电子研究所,天津 300072)

摘 要: 在铌酸锂晶体非共线相位匹配太赫兹波参量振荡器中观察到了级联光学参量效应。实验中测量到了一阶、二阶和三阶斯托克斯光。通过分析一阶、二阶和三阶斯托克斯光谱发现相邻阶斯托克斯光频率差相等,表明在太赫兹波的产生过程中发生了级联光学参量效应。在高阶级联光学参量过程中,一个泵浦光子可以产生多个太赫兹光子,表明在太赫兹波产生过程中量子转换效率会有效提高。

关键词: 太赫兹波; 太赫兹波参量振荡器; 级联光学参量振荡

收稿日期:2014−07−22; **修订日期:**2014−08−26

基金项目:国家自然科学基金(61201101,61205003)

作者简介:李忠洋(1983−),男,副教授,博士,主要从事非线性光学产生太赫兹波方面的研究。Email:thzwave@163.com

0 Introduction

Terahertz (THz) radiation, widely defined as electromagnetic radiation in the frequency range 0.1–10 THz, offers researchers many intriguing possibilities, ranging from fundamental science through to applications in communications, imaging and spectroscopy, security and defense, and non-destructive evaluation[1-6]. Among many electronic and optical methods for the THz-wave generation, THz-wave parametric oscillator (TPO) and difference-frequency generation (DFG) in a second-order nonlinear medium exhibit many advantages, such as narrow linewidth, coherent, wide tunable range, high-power output and room temperature operation[7-9]. The TPO with both noncollinear phase-matching configuration and quasi-phase-matching configuration can perform well[10-11]. Unfortunately, the quantum conversion efficiency of the TPO and DFG is extremely low as the THz-wave is intensely absorbed by the gain medium. To improve the low quantum conversion efficiency, Sowade et al. present a continuous-wave optical parametric terahertz light source with a scheme of cascaded processes which can increases the output power of a terahertz system by more than one order of magnitude[12]. Walsh et al. report the use of quasi-phase-matching techniques based on periodically-poled MgO:$LiNbO_3$ with a scheme of cascaded difference frequency generations for the generation of nanosecond duration pulses of terahertz radiation in intracavity optical parametric oscillators[13]. Liu et al. analyze the threshold and conversion efficiency of a cascaded continuous-wave TPO[14]. With high-order cascaded parametric processes one pump photon can generate several THz photons, suggesting that the overall quantum conversion efficiency for the THz radiation can overcome the Manley-Rowe limit.

In this paper, we report on the observation of the high-order Stokes waves from cascaded parametric processes with a noncollinear phase-matching scheme. We present a comprehensive study of the effect.

1 Experimental setup and results

The experimental setup comprised a single-resonant optical parametric oscillator with a Fabry-Perot cavity pumped by a multi-longitudinal-mode Q-switched Nd:YAG laser at 1064 nm, as shown in Fig.1.

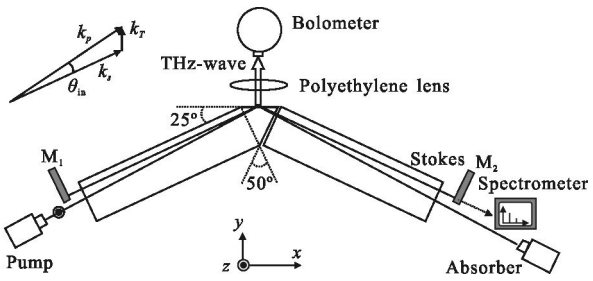

Fig.1 Experimental setup of the MgO:$LiNbO_3$-TPO. Fabry-perot cavity and the MgO:LiNbO3 crystal are mounted onto a rotating stage

The pulse width and the repetition rate of the pump wave were 15 ns and 10 Hz, respectively. The pump beam was collimated by a lens pair to a diameter of about 1.9 mm. The nonlinear gain mediums were composed of two 5 mol% MgO doped $LiNbO_3$ crystals. The dimensions of the rectangular crystal were $50(x)\times10(y)\times5(z)$ mm^3. The other pentagonal crystal was composed of a rectangular crystal with dimensions of $50(x)\times10(y)\times5(z)$ mm^3 and an isosceles triangle crystal with an apex angle of 50°. The incident angle of the Stokes wave to the exit facet of the THz-wave was 65°, which ensured that the THz-wave almost perpendicularly exited from the $LiNbO_3$ crystal due to noncollinear phase matching condition. All the crystal surfaces were antireflection coated with a residual reflectivity smaller than 1% at the Stokes wavelengths. The polarizations of the pump wave, Stokes wave and THz-wave were all along the z-axis of the $LiNbO_3$ crystal. The TPO cavity for the Stokes wave consisted of two plane-parallel mirrors, M_1 and M_2. M_1 was highly reflecting (>99.8%) and M_2 was coated with a reflectivity of 85%. The cavity with a length of 210 mm was symmetric. The pump wave passed through the

cavity at the edge of M_1 and M_2. The cavity mirrors and the MgO:$LiNbO_3$ crystal were mounted on a rotating stage. The wavelength of the first-order Stokes wave, and hence the wavelength of the THz-wave can be tuned by rotating the stage continuously since the angle between the pump wave vector and the optical axis of the Stokes wave cavity are changing continuously.

By using a single optical fiber positioned beyond M_2, feeding into an optical spectrum analyzer (Agilent, model 86142B), the wavelengths of the high-order Stokes waves can be measured. During the experiments we observe the spectra of the pump wave, the first-, second-, and third-order Stokes waves, as shown in Fig.2. The wavelengths of the pump wave, the first-, second-, and third-order Stokes waves are 1064.44 nm, 1071.35 nm, 1078.36 nm and 1085.45 nm, respectively. The frequency difference of 1.818 THz between the pump wave and the first-order Stokes wave immediately gives the frequency of the THz-wave generated by the first-order parametric process. The difference frequencies between the first-order and the second-order Stokes wave, the second-order and the third-order Stokes wave are 1.820 THz and 1.817 THz, respectively. The spectral lines exhibit a constant frequency shift between the adjacent-order Stokes waves.

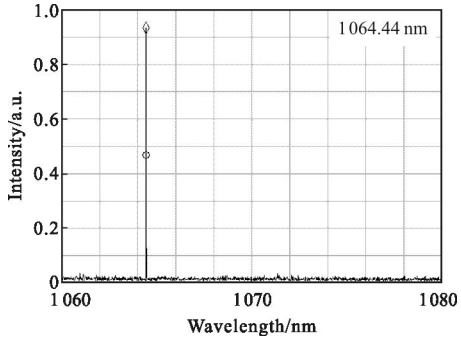

(a) Pump wave

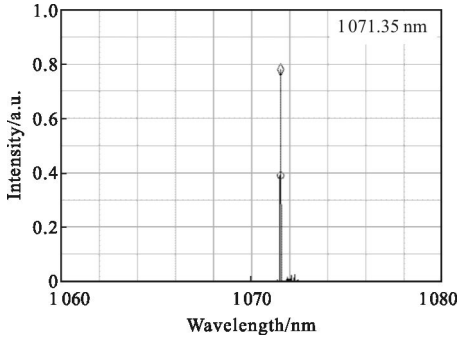

(b) First-order Stokes wave

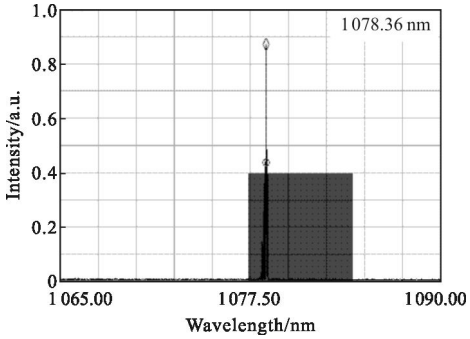

(c) Second-order Stokes wave

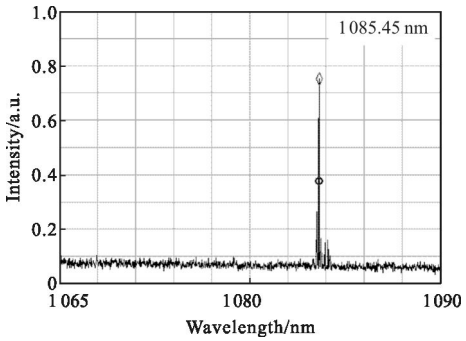

(d) Third-order Stokes wave

Fig.2 Spectra of the pump wave and stokes waves captured by an agilent 86142B optical spectrum analyzer

2 Investigation of the high-order Stokes waves

The near equality of the frequency differences mentioned above is consistent with the second-order Stokes wave being generated by the process of DFG in which the THz-wave, which is parametrically generated as a result of the interaction between the pump-wave and the first-order Stokes wave, then subsequently interacts with the first-order Stokes wave so as to generate the second-order Stokes wave. The cascaded optical processes can be continued as the high-power and high conversion efficiency THz-wave radiations based on DFG have been realized[15-17]. The energy diagram and phase-matching diagram of cascaded optical parametric processes is shown in Fig.3. The first-order parametric process converts the pump

wave ω_p into the THz−wave ω_T and the first-order Stokes wave ω_{s1}. The second-order Stokes wave ω_{s2} is generated by the process of DFG in which the first-order Stokes wave ω_{s1} interacts with the THz−wave ω_T. The THz−wave ω_T which is initially generated in the first-order parametric process is amplified within the process of DFG. The third-order Stokes wave ω_{s3} is generated by the process of DFG in which the THz−wave ω_T interacts with the second-order Stokes wave ω_{s2}. With high-order cascaded optical parametric processes from every pump photon several terahertz photons are created rather than only one.

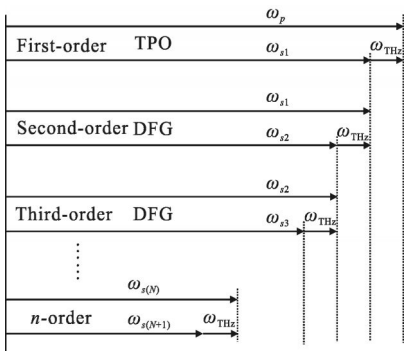

(a) Energy diagram of cascaded optical parametric processes

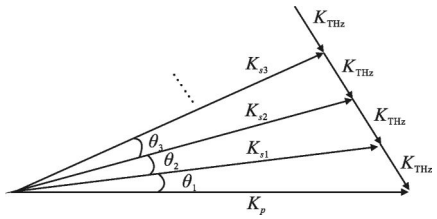

(b) Phase-matching diagram of cascaded optical parametric processes (The lengths of the wavevectors do not scale)

Fig.3 Cascaded optical parametric processes

The propagation direction of the first-order Stokes wave is determined by the optical axis of the Stokes wave resonant cavity formed by mirrors M_1 and M_2. The propagation direction of the second-order and third-order Stokes wave is undefined by any external constraints, and is determined by the phase matching condition alone, as shown in Fig.3 (b). For the first-order THz−wave parametric process, two requirements have to be fulfilled: the energy conservation condition:

$$\frac{1}{\lambda_p}=\frac{1}{\lambda_{s1}}+\frac{1}{\lambda_T} \tag{1}$$

and the phase-matching condition:

$$\vec{k}_p=\vec{k}_{s1}+\vec{k}_T \tag{2}$$

Here, λ is the wavelength, while $\vec{k}$ is the wave-vector, the subscripts p, $s1$ and T denote the pump wave, first-order Stokes wave and THz−wave, respectively. The magnitudes of the corresponding wave vectors (within the nonlinear gain medium) are calculated using the following equation:

$$k_j=\frac{2\pi n_j}{\lambda_j} \tag{3}$$

where the subscript j indicates the wave of interest, and n_j is the refractive index for that wave. The phase-matching condition can be rewritten as

$$k_T^2=k_p^2+k_{s1}^2-2k_pk_{s1}\cos\theta_1 \tag{4}$$

where θ_1 is the angle between the pump wave and the first-order Stokes wave.

For the second-order process, the energy conservation condition is

$$\frac{1}{\lambda_{s1}}=\frac{1}{\lambda_{s2}}+\frac{1}{\lambda_T} \tag{5}$$

and the phase-matching condition is

$$k_T^2=k_{s1}^2+k_{s2}^2-2k_{s1}k_{s2}\cos\theta_2 \tag{6}$$

Here, the subscript $s2$ denotes the second-order Stokes waves. θ_2 is the angle between the first-order Stokes wave and the second-order Stokes wave.

For the third-order process, the energy conservation condition is

$$\frac{1}{\lambda_{s2}}=\frac{1}{\lambda_{s3}}+\frac{1}{\lambda_T} \tag{7}$$

and the phase-matching condition is

$$k_T^2=k_{s2}^2+k_{s3}^2-2k_{s2}k_{s3}\cos\theta_3 \tag{8}$$

Here, the subscript $s3$ denotes the third-order Stokes waves. θ_3 is the angle between the second-order Stokes wave and the third-order Stokes wave.

The theoretical values of the pump and Stokes wavelengths are calculated using a wavelength- and temperature-independent Sellmeier equation for 5% MgO−doped congruent lithium niobate (MgO:cLN) in

the IR[18] and THz range, respectively[19]. The Sellmeier equation for MgO:cLN of Gayer et al[18]. in the IR range in a temperature range from 20 ℃ to 200 ℃ can be written as

$$n_e^2=a_1+b_1f+\frac{a_2+b_2f}{\lambda^2-(a_3+b_3f)^2}+\frac{a_4+b_4f}{\lambda^2-a_5}-a_6\lambda^2 \tag{9}$$

where a_1=5.756, a_2=0.0983, a_3=0.202, a_4=189.32, a_5=12.52, a_6=1.32×10^{-2}, b_1=2.86×10^{-6}, b_2=4.7×10^{-8}, b_3=6.113×10^{-8}, b_4=1.516×10^{-4}, and $f=(T-24.5)\times(T+570.82)$, T is the crystal temperature in ℃. The Sellmeier equation for MgO:cLN of Kiessling et al[19]. in the THz range in a temperature range from 30 ℃ to 200 ℃ can be written as

$$n_{\mathrm{THz}}^2=A_0+B_0f+\frac{A_1+B_1f}{\lambda^2-(A_2+B_2f)^2} \tag{10}$$

where A_0=24.326, A_1=31298, A_2=48.084, B_0=2.14×10^{-5}, B_1=0.15824, B_2=−3.097×10^{-4}.

According to the Eqs.(4)–(8), the frequency tuning of the first−, second−, third-order Stokes waves can be realized by varying the angle θ_1 between the pump wave and the first-order Stokes wave, as is shown in Fig.4. The insert symbols are the experimental values. We measure 8 groups of experimental value at different angles θ_1. From the figure we find that the experimental values agree well with the theoretical values calculated from the cascaded parametric processes. At any angle θ_1 the frequency difference between the first-order and second-order Stokes waves is approximately equal to the difference between the second-order and third-order Stokes waves, which means that the high-order cascaded parametric processes have realized.

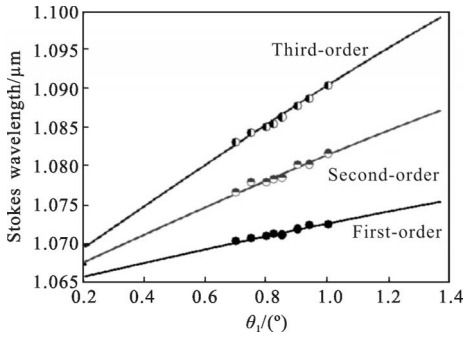

Fig.4 Wavelengths of the first−, second−, third-order Stokes waves versus the angle θ_1 (The solid lines show theoretical values, the symbols are measured values)

In contrast to the use of PPLN for THz−wave generation in the collinear phase-matching scheme, the use of bulk lithium niobate in the noncollinear phase-matching scheme is convenient for the generation of the tuning THz−wave by tuning the phase-matching angle between the pump wave and the first-order Stokes wave.

3 Conclusion

Cascaded optical parametric processes in terahertz parametric oscillator with a noncollinear phase-matching scheme based on bulk lithium niobate are observed. By analyze the spectra of the first−, second−, and third-order Stokes waves we find that the first-order parametric process is optical parametric oscillation and the high-order parametric processes are difference frequency generation. The frequency difference between adjacent-order Stokes waves is approximately equivalent. With high-order cascaded terahertz parametric processes one pump photon can generate several THz photons.

References:

[1] Su J P, Ma F Y, Yu Z F, et al. Theoretical design of terahertz-wave parametric oscillator based on $LiNbO_3$ crystal [J]. ***Infrared and Laser Engineering***, 2010, 39(3): 482−486. (in Chinese)

[2] Lu Y M, Wang J C, Shi J M, et al. Application of THz technology for detection in soot and wind-blown sand [J]. ***Infrared and Laser Engineering***, 2010, 39 (3):487−490. (in Chinese)

[3] Abbott D, Zhang X C. T−ray imaging, sensing, and retection [J]. ***IEEE***, 2007, 95(8): 1509−1513.

[4] Melnick G J, Stauffer J R, Ashby M L N, et al. The submillimeter wave astronomy satellite: Science objectives and instrument description[J]. ***Astrophys J Lett***, 2000, 539(2): L77−L85.

[5] Kleine-Ostmann T, Nagatsuma T. A review on terahertz communications research[J]. ***Journal of Infrared, Millimeter,***

and Terahertz Waves, 2001, 32(2): 143−171.

[6] Oh S J, Kang J, Maeng I, et al. Nanoparticle-enabled terahertz imaging for cancer diagnosis[J]. ***Opt Express***, 2009, 17(5): 3469−3475.

[7] Kawase K, Shikata J, Ito H. Terahertz wave parametric source [J]. ***J Phys D: Appl Phys***, 2002, 35: R1−R14.

[8] Shi W, Ding Y J. A monochromatic and high-power THz source tunable in the ranges of 2.7−38.4 um and 58.2−3540 um for variety of potential applications [J]. ***Appl Phys Lett***, 2004, 84(10): 1635−1637.

[9] Zhao, P Ragam S, Ding Y J, et al. Singly resonant optical parametric oscillator based on adhesive-free-bonded periodically inverted $KTiOPO_4$ plates: terahertz generation by mixing a pair of idler waves[J]. ***Opt Lett***, 2012, 37(7): 1283−1285.

[10] Ikari T, Zhang X, Minamide H, et al. THz−wave parametric oscillator with a surface-emitted configuration [J]. ***Opt Express***, 2006, 14(4): 1604−1610.

[11] Molter D, Theuer M, Beigang R. Nanosecond terahertz optical parametric oscillator with a novel quasi phase matching scheme in lithium niobate [J]. ***Opt Express***, 2009, 17(8): 6623−6628.

[12] Sowade R, Breunig I, Mayorga I C, et al. Continuous-wave optical parametric terahertz source [J]. ***Opt Express***, 2009, 17(25): 22303−22310.

[13] Walsh D A, Browne P G, Dunn M H, et al. Intracavity parametric generation of nanosecond terahertz radiation using quasi-phase-matching[J]. ***Opt Express***, 2010, 18(13): 13951−13963.

[14] Liu L, Li X, Xu X J, et al. Theoretical analysis of a cascaded continuous-wave optical parametric oscillator [J]. ***Journal of Infrared, Millimeter, and Terahertz Waves***, 2013, 34(3): 238−250.

[15] Shi W, Ding Y J, Fernelius N, et al. An efficient, tunable, and coherent 0.18−5.27 THz source based on GaSe crystal [J]. ***Opt Lett***, 2002, 27(16): 1454−1456.

[16] Xu G, Mu X, Ding Y J, et al. Efficient generation of backward terahertz pulses from multiperiod periodically-poled lithium niobate [J]. ***Opt Lett***, 2009, 34(7): 995−997.

[17] Jiang Y, Li D, Ding Y J, et al. Terahertz generation based on parametric conversion: from saturation of conversion efficiency to back conversion [J]. ***Opt Lett***, 2011, 36 (9): 1608−1610.

[18] Gayer O, Sacks Z, Galun E, et al. Temperature and wavelength dependent refractive index equations for MgO−doped congruent and stoichiometric $LiNbO_3$[J]. ***Appl Phys B: Lasers Opt***, 2008, 91(2): 343−348.

[19] Kiessling J, Buse K, Breunig I. Temperature-dependent Sellmeier equation for the extraordinary refractive index of 5 mol.% MgO−doped $LiNbO_3$ in the terahertz range [J]. ***J Opt Soc Am B***, 2013, 30(4): 950−952.